Received 20 February; accepted 6 March 2001.

1. Nagamatsu, J., Nakagawa, N., Muranaka, T., Zenitani, Y. & Akimitsu, J. Superconductivity at 39 K in magnesium diboride. *Nature* **410,** 63–64 (2001).
2. Cohen, L. F. & Jensen, H. J. Open questions in the magnetic behaviour of high temperature superconductors. *Rep. Prog. Phys.* **60,** 1581–1672 (1997).
3. Mannhart, J., Chaudhari, P., Dimos, D., Tsuei, C. C. & McGuire, T. R. Critical currents in [001] grains and across their tilt boundaries in $YBa_2Cu_3O_7$ films. *Phys. Rev. Lett.* **61,** 2476–2479 (1988).
4. Miyakawa, N. *et al.* Predominantly superconducting origin of large energy gaps in underdoped $Bi_2Sr_2CaCu_2O_{8+}$ from tunneling spectroscopy. *Phys. Rev. Lett.* **83,** 1018–1021 (1999).
5. Cucolo, A. M. *et al.* Quasiparticle tunneling properties of planar $YBa_2Cu_3O_{7-\delta}/PrBa_2Cu_3O_{7-\delta}/HoBa_2Cu_3O_{7-\delta}$ heterostructures. *Phys. Rev. Lett.* **76,** 1920–1923 (1996).
6. Caplin, A. D., Cohen, L. F., Perkins, G. K. & Zhukov, A. A. The electric-field within high-temperature superconductors—mapping the *E-J-B* surface. *Supercond. Sci. Technol.* **7,** 412–422 (1994).
7. Larbalestier, D. C. *et al.* Strongly linked current flow in polycrystalline forms of the superconductor MgB_2. *Nature* **410,** 186–189 (2001).
8. Finnemore, D. K., Ostenson, J. E., Bud'ko, S. L., Lapertot, G. & Canfield, P. C. Thermodynamic and transport properties of superconducting MgB_2. Preprint cond-mat/0102114 at ⟨http://xxx.lanl.gov⟩ (2001).
9. Takano, Y. *et al.* Superconducting properties of MgB_2 bulk materials prepared by high pressure sintering. Preprint cond-mat/0102167 at ⟨http://xxx.lanl.gov⟩ (2001).
10. Pust, L., Jirsa, M. & Durcok, S. Correlation between magnetic hysteresis and magnetic-relaxation in YBaCuO single-crystals. *J. Low Temp. Phys.* **78,** 179–186 (1990).
11. Perkins, G. K. & Caplin, A. D. Collective pinning theory and the observed vortex dynamics in $(RE)Ba_2Cu_3O_{7-\delta}$ crystals. *Phys. Rev. B* **54,** 12551–12556 (1996).
12. Canfield, P. C. *et al.* Superconductivity in dense MgB_2 wires. Preprint cond-mat/0102289 at ⟨http://xxx.lanl.gov⟩ (2001).
13. Bean, C. P. Magnetization of high-field superconductors. *Rev. Mod. Phys.* **36,** 31–36 (1964).

Acknowledgements

Y.B. is on leave of absence from the General Physics Institute, Moscow, Russia. We thank D. Cardwell and N. H. Babu for the supply of MgB_2 powder, and A. J. P. White for crystallographic advice. This work was supported by the UK Engineering and Physical Sciences Research Council.

Correspondence and requests for materials should be addressed to Y.B. (e-mail: y.bugoslav@ic.ac.uk).

Extreme damping in composite materials with negative-stiffness inclusions

R. S. Lakes*†‡§‖, T. Lee‡, A. Bersie*† & Y. C. Wang*†

** Department of Engineering Physics; † Engineering Mechanics Program; ‡ Biomedical Engineering Department; § Materials Science Program; and ‖ Rheology Research Center, University of Wisconsin-Madison, 147 Engineering Research Building, 1500 Engineering Drive, Madison, Wisconsin 53706-1687, USA*

When a force deforms an elastic object, practical experience suggests that the resulting displacement will be in the same direction as the force. This property is known as positive stiffness[1]. Less familiar is the concept of negative stiffness, where the deforming force and the resulting displacement are in opposite directions. (Negative stiffness is distinct from negative Poisson's ratio[2–6], which refers to the occurrence of lateral expansion upon stretching an object.) Negative stiffness can occur, for example, when the deforming object has stored[7] (or is supplied[8] with) energy. This property is usually unstable, but it has been shown theoretically[9] that inclusions of negative stiffness can be stabilized within a positive-stiffness matrix. Here we describe the experimental realization of this composite approach by embedding negative-stiffness inclusions of ferroelastic vanadium dioxide in a pure tin matrix. The resulting composites exhibit extreme mechanical damping and large anomalies in stiffness, as a consequence of the high local strains that result from the inclusions deforming more than the composite as a whole. Moreover, for certain temperature ranges, the negative-stiffness inclusions are more effective than diamond inclusions for increasing the overall composite stiffness. We expect that such composites could be useful as high damping materials, as stiff structural elements or for actuator-type applications.

Composite materials were prepared with inclusions of vanadium dioxide (VO_2) in a pure (99.99%) tin matrix. Particulate inclusions 150 μm in size or smaller were incorporated into a tin matrix by rolling sheets of tin with particles, followed by casting into a cylindrical mould 3 mm in diameter. Vanadium dioxide is a ferroelastic material[10–12] that undergoes a transformation from monoclinic to tetragonal at transformation temperature $T_c = 67\,^{\circ}C$; the transition exhibits hysteresis. It is similar in structure[10] to the stiff mineral rutile (TiO_2) with elastic moduli[13] $C_{11} = 271$ GPa and $C_{33} = 483$ GPa. By contrast, steel has a Young's modulus of $E = 200$ GPa ($C_{11} = C_{33} = 269$ GPa); for tin $E = 50$ GPa.

The material properties were measured using a broadband viscoelastic spectroscopy apparatus[14,15], capable of a range of eleven decades of time and frequency in torsion. Specimens were mounted using cyanoacrylate cement: at the top to its support rod, and at the bottom, to a high magnetic intensity neodymium iron boron magnet. The dynamic experiments were conducted by applying a sinusoidal voltage at 100 Hz, from a digital function generator to a Helmholtz coil. The lowest specimen resonance was at several kilohertz. The coil imposed a magnetic field on the permanent magnet and transmitted an axial torque to the specimen. The angular displacement of the specimen was measured using laser light reflected from a mirror mounted on the magnet to a split-diode light detector. The detector signal was amplified with a wide-band differential amplifier. Torque was inferred from the Helmholtz coil current, supported by calibrations using the well characterized 6061 Al alloy[29]. Input and output voltages and the phase between them were recorded using a lock-in amplifier (SRS 850, Stanford Research Systems). Data were reduced using the analytical relationship for the torsional rigidity of a viscoelastic cylinder. Constituent stiffness was tuned by varying the temperature. An insulated inner chamber was heated to above 85 °C and the temperature was maintained for at least 30 minutes. The heater was shut off and the chamber allowed to cool. Cooling rate over the temperature range of interest was less than 1 °C per minute.

Material properties, stiffness and damping (tanδ, where δ is the phase between stress and strain) as a function of temperature of a particulate VO_2–tin composite with 1% by volume of inclusions are shown in Fig. 1. Although the concentration of inclusions is dilute, large anomalies are observed in the mechanical damping, tanδ, as well as in the stiffness. For comparison, tanδ of pure Sn is 0.019 and varies little with temperature, as shown. The sharp dependence on temperature we attribute to the fact that the inclusions are much stiffer than the matrix (away from the transition temperature) and can only balance the matrix stiffness near the transition. The peaks observed in the present 1% VO_2 composite are larger than in 100% VO_2, which had a peak[12] of 0.04 to 0.05 in tanδ and a dip of 8% in stiffness at the transition. In the composite, there is interplay between constituents of positive and negative stiffness; by contrast, 100% VO_2 has positive stiffness at all temperatures due to the formation of domains.

A negative-stiffness lumped element (a structure) can be stabilized by a hard constraint. For an unconstrained block (or, surface traction boundary condition, in the language of elasticity[1]) of isotropic material to be stable, the shear modulus G and the bulk modulus B, as stiffness quantities, must be positive. This corresponds to a range of Poisson's ratio ν (defined as the negative transverse strain of a stretched or compressed body divided by its longitudinal strain) $-1 < \nu < 0.5$. Materials of negative Poisson's ratio, while exhibiting the unusual property of transverse expansion when stretched, can have all positive-stiffness values, and hence stability. For most solids[1], ν is between 0.25 and 0.33.

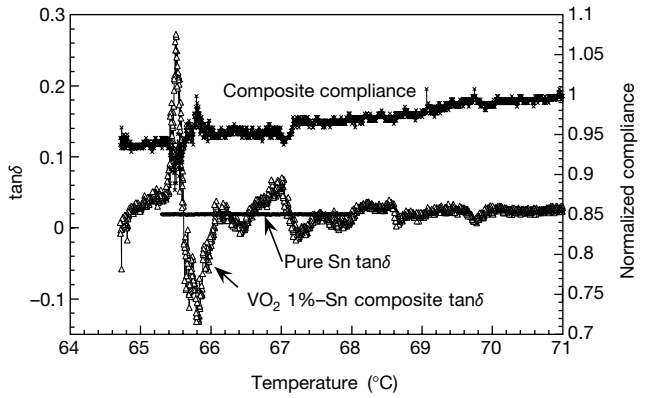

Figure 1 Experimental torsional compliance (inverse stiffness) and mechanical damping, tanδ, versus temperature. Open triangles show damping of a composite containing 1% by volume vanadium dioxide particles in a tin matrix. Crossed points show damping of pure tin for which tanδ = 0.019 over the temperature range considered. Measurements were conducted at 100 Hz, well below resonance, during slow cooling through the ferroelastic transition of the inclusions.

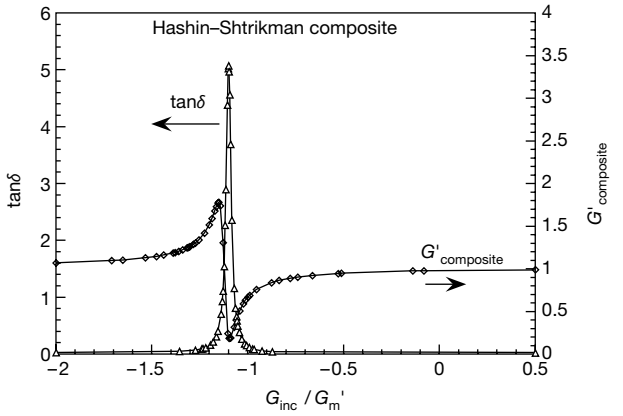

Figure 2 Theoretical shear modulus G' (real part) and mechanical damping, tanδ, versus inclusion shear modulus G_{inc} normalized to matrix shear modulus G'_m, of Hashin–Shtrikman composite containing 1% of spherical particulate inclusions by volume. Inclusions are allowed to have a negative shear modulus. Matrix damping is assumed to be 0.025. Inclusion damping is assumed to be zero. Similar behaviour is predicted in the bulk properties if the inclusions have a negative bulk modulus.

Foams[2,3] with $\nu \approx -0.7$, and polycrystals[4], crystals[6], and other microstructures[5] with a negative Poisson's ratio have been produced; they are stable. For a constrained isotropic block (surface displacement boundary condition[16]), stability requires $G > 0$ and $-\infty < \nu < 0.5$ or $1 < \nu < \infty$. As Young's modulus is $E = 2G(1+\nu)$, an isotropic material with Young's modulus less than zero is stable provided it is constrained. Another criterion of stability is strong ellipticity[17], for which $G > 0$ and $\nu < 0.5$ or $\nu > 1$, allowing negative Young's and bulk moduli. Violation of strong ellipticity gives rise to instability: bands of heterogeneous deformation[17] form in materials. In single domains of ferroelastic material, band formation is suppressed by surface energy considerations. Therefore single domain particles, when constrained by a sufficiently stiff composite matrix, can be stable. So inclusions can have negative Young's modulus, and if they are small enough, even negative shear modulus.

The stabilizing constraint need not be perfectly rigid; it can be the matrix phase of a composite. Specifically, we have shown[9] via composite theory that negative-stiffness elastic materials can be stabilized by embedding them as polydisperse spherical inclusions in an isotropic composite governed by the Hashin–Shtrikman shear modulus (G_L) formula[18]

$$G_L = G_2 + \frac{V_1}{\dfrac{1}{G_1 - G_2} + \dfrac{6(K_2 + 2G_2)V_2}{5(3K_2 + 4G_2)G_2}} \qquad (1)$$

where K_1 and K_2, G_1 and G_2, and V_1 and V_2 are the bulk modulus, shear modulus and volume fraction of phases 1 and 2, respectively. Although we can show that a system is stable with respect to certain modes of instability, we cannot confidently prove that a complex system is stable with respect to all possible modes, of which there may be an infinite number. Therefore experiments are necessary.

For viscoelastic materials, the moduli become complex following the elastic–viscoelastic correspondence principle[19,20]. When inclusion phase 1 has a negative shear modulus of about −1.1 of the matrix modulus, composite behaviour[21] is predicted to exhibit a large peak in damping, tanδ, and an anomaly in stiffness. As an illustration of the concept, Fig. 2 shows representative behaviour versus inclusion stiffness based on composite theory with isotropic inclusions and matrix. The abscissa is normalized inclusion stiffness, which is tuned indirectly by temperature in the experiments. If inclusion concentration is increased or matrix damping is reduced, theory allows the composite to have negative stiffness and tanδ. The theory is simplistic in that inclusion anisotropy and heterogeneity of their environment is ignored.

Indirect experimental evidence of negative shear modulus is found in the banding instability which occurs in compressed foams[22]. In ferroelastic, ferroelectric and ferromagnetic materials[23] the bands, called domains, occur below a transformation temperature T_c. Small particles may be single domains[23], owing to surface energy; domain size can be from micrometres to centimetres depending on the material. A negative-stiffness material may be represented by an energy versus deformation diagram in which there are at least two relative minima or energy wells. Negative stiffness was directly observed experimentally in tetrakaidecahedral single-cell models of foam materials, in compression under displacement control constraint[22]. The concept of composites with negative stiffness is supported by experimental study of a constrained, lumped one-dimensional model system involving a single buckled tube as a negative stiffness element[24].

Observed stiffness and damping anomalies in the composite are much larger than they could be for inclusions of any positive stiffness or damping. For example, if the particles were as stiff as diamond ($E = 1{,}000$ GPa), composite theory[18] predicts a composite stiffening effect of only 1.9% and no change in tanδ; if the particles were infinitely stiff, the composite would be only 2.1% stiffer than a tin matrix. If the particle stiffness were to vanish, the composite would soften by 1.9% and have no change in tanδ. The inclusions are therefore more effective than diamond in increasing the composite stiffness at selected temperatures; moreover, the composite exceeds the classical bounds[18] based on positive stiffness. The observed peaks in damping cannot be explained by any variation in the properties of positive-stiffness inclusions. Even if inclusion tanδ were as large as 1.0 at the transition, composite damping could increase from 0.025 to at most 0.032, assuming positive inclusion stiffness. Therefore the inclusions exhibit negative stiffness.

Composites with inclusions of negative stiffness may be called exterlibral because they are on the boundary of balance, or archidynamic because they are based on initial force. They are pertinent to any heterogeneous material in which one constituent undergoes a phase transformation and another does not; also to some materials with a pre-strained constituent. They may be of use in studying the properties of single domains of ferroelastic, ferroelectric, ferromagnetic, or shape memory martensite[25] materials. Because a dilute concentration is sufficient to obtain substantial effects, not much sample material is needed. Some materials can be easily prepared as

large single crystals; polycrystalline arrays may be brittle. Such composites may be of use as high-performance damping materials, since the figure of merit[26] in the present results exceeds that of commonly used materials ($E\tan\delta \approx 0.6$ GPa) by a factor of more than 20. For that purpose, sensitivity to temperature could be reduced via matching inclusion and matrix stiffness. Moreover, pre-stressed or pre-buckled[24] elements with minimal temperature sensitivity may be used as inclusions. Bounds on properties of complex heterogeneous materials are generally derived assuming positive phase properties[18]. These bounds can be exceeded if negative stiffness is allowed, permitting extreme properties not previously anticipated. As in thermoelastic and piezoelectric materials, elasticity is coupled with temperature and electric field respectively, these composites may find use in high-performance sensors and actuators. These composites may also occur naturally in rocks and in biological materials (in which anomalies were reported[27]); they may be considered in the context of deep-focus earthquakes and attenuation of seismic waves. □

Received 25 July 2000; accepted 2 February 2001.

1. Timoshenko, S. P. & Goodier, J. N. *Theory of Elasticity* 3rd edn (McGraw-Hill, New York, 1970).
2. Lakes, R. S. Foam structures with a negative Poisson's ratio. *Science* **235,** 1038–1040 (1987).
3. Lakes, R. S. Advances in negative Poisson's ratio materials. *Adv. Mater.* **5,** 293–296 (1993).
4. Haeri, A. Y., Weidner, D. J. & Parise, J. B. Elasticity of α-cristobalite: a silicon dioxide with a negative Poisson's ratio. *Science* **257,** 650–652 (1992).
5. Rothenburg, L., Berlin, A. A. & Bathurst, R. J. Microstructure of isotropic materials with negative Poisson's ratio. *Nature* **354,** 470–472 (1991).
6. Baughman, R. H., Shacklette, J. M., Zakhidov, A. A. & Stafstrom, S. Negative Poisson's ratios as a common feature of cubic metals. *Nature* **392,** 362–365 (1998).
7. Thompson, J. M. T. Stability prediction through a succession of folds. *Phil. Trans. R. Soc. Lond.* **292,** 1–23 (1979).
8. Thompson, J. M. T. 'Paradoxical' mechanics under fluid flow. *Nature* **296,** 135–137 (1982).
9. Lakes, R. S. & Drugan, W. J. Stiff elastic composite materials with a negative stiffness phase. *J. Mech. Phys. Solids* (submitted).
10. Heckingbottom, R. & Linnett, J. W. Structure of vanadium dioxide. *Nature* **194,** 678 (1962).
11. Paquet, D. & Leroux-Hagon, P. Electron correlations and electron-lattice interactions in the metal-insulator ferroelastic transition in VO_2: a thermodynamical study. *Phys. Rev. B* **22,** 5284–5301 (1979).
12. Zhang, J. X., Yang, Z. H. & Fung, P. C. W. Dissipation function of the first-order phase transformation in VO_2 ceramics by internal friction measurements. *Phys. Rev. B* **52,** 278–284 (1995).
13. *Handbook of Chemistry and Physics* C-40 12–40 (CRC Press, Boca Raton, Florida, 1996).
14. Brodt, M., Cook, L. S. & Lakes, R. S. Apparatus for measuring viscoelastic properties over ten decades: refinements. *Rev. Sci. Instrum.* **66,** 5292–5297 (1995).
15. Lakes, R. S. & Quackenbush, J. Viscoelastic behaviour in indium tin alloys over a wide range of frequency and time. *Phil. Mag. Lett.* **74,** 227–232 (1996).
16. Bramble, J. H. & Payne, L. E. On the uniqueness problem in the second boundary value problem in elasticity. *Proc. 4th Natl Cong. Appl. Mech.* 469–473 (American Society of Mechanical Engineers, Berkeley, California, 1963).
17. Knowles, J. K. & Sternberg, E. On the failure of ellipticity and the emergence of discontinuous gradients in plane finite elastostatics. *J. Elasticity* **8,** 329–379 (1978).
18. Hashin, Z. & Shtrikman, S. A variational approach to the theory of the elastic behavior of multiphase materials. *J. Mech. Phys. Solids* **11,** 127–140 (1963).
19. Read, W. T. Stress analysis for compressible viscoelastic materials. *J. Appl. Phys.* **21,** 671–674 (1950).
20. Hashin, Z. Viscoelastic behavior of heterogeneous media. *J. Appl. Mech. Trans. ASME* **32E,** 630–636 (1965).
21. Lakes, R. S. Extreme damping in composite materials with a negative stiffness phase. *Phys. Rev. Lett.* (in the press).
22. Rosakis, P., Ruina, A. & Lakes, R. S. Microbuckling instability in elastomeric cellular solids. *J. Mater. Sci.* **28,** 4667–4672 (1993).
23. Salje, E. *Phase Transitions in Ferroelastic and Co-elastic Crystals* 10, 72 (Cambridge Univ. Press, Cambridge, 1990).
24. Lakes, R. S. Extreme damping in compliant composites with a negative stiffness phase. *Phil. Mag. Lett.* **81,** 95–100 (2001).
25. Ren, X. & Otsuka, K. Origin of rubber-like behaviour in metal alloys. *Nature* **389,** 579–583 (1997).
26. Cremer, L., Heckl, M. A. & Ungar, E. E. *Structure Borne Sound* 2nd edn 243–247 (Springer, Berlin, 1988).
27. Pugh, J. W., Rose, R. M., Paul, I. L. & Radin, E. L. Mechanical resonance spectra in human cancellous bone. *Science* **181,** 271–272 (1973).
28. Falk, F. Model free energy, mechanics, and thermodynamics of shape memory alloys. *Acta Metall.* **28,** 1773–1780 (1980).
29. Duffy, W. Acoustic quality factor of aluminum alloys from 50 mK to 300 K. *J. Appl. Phys.* **68,** 5601–5609 (1990).

Acknowledgements

We thank W. Drugan and R. Cooper for supportive comments and discussions. This work was supported by the NSF.

Correspondence and requests for materials should be addressed to R.S.L. (e-mail: lakes@engr.wisc.edu).

Climate variability 50,000 years ago in mid-latitude Chile as reconstructed from tree rings

Fidel A. Roig*, Carlos Le-Quesne†‡, José A. Boninsegna*, Keith R. Briffa§, Antonio Lara‡, Håkan Grudd‖, Philip D. Jones§ & Carolina Villagrán¶

* *Laboratorio de Dendrocronología, IANIGLA-CONICET, CC 330 (5500) Mendoza, Argentina*
† *Department Botánica, Facultad de Biología, Universidad de Oviedo, Catedrático Rodrigo Uría s/n, 33006, Spain*
‡ *Instituto de Silvicultura, Universidad Austral de Valdivia, Casilla 567, Valdivia, Chile*
§ *Climate Research Unit, School of Environmental Sciences, University of East Anglia, Norwich NR4 7TJ, UK*
‖ *Department of Physical Geography, Stockholm University, S-10691 Stockholm, Sweden*
¶ *Department Biología, Facultad de Ciencias, Universidad de Chile, Casilla 653, Santiago, Chile*

High-resolution proxies of past climate are essential for a better understanding of the climate system[1]. Tree rings are routinely used to reconstruct Holocene climate variations at high temporal resolution[2], but only rarely have they offered insight into climate variability during earlier periods[3]. *Fitzroya cupressoides*—a South American conifer which attains ages up to 3,600 years—has been shown to record summer temperatures in northern Patagonia during the past few millennia[4]. Here we report a floating 1,229-year chronology developed from subfossil stumps of *F. cupressoides* in southern Chile that dates back to approximately 50,000 ^{14}C years before present. We use this chronology to calculate the spectral characteristics of climate variability in this time, which was probably an interstadial (relatively warm) period. Growth oscillations at periods of 150–250, 87–94, 45.5, 24.1, 17.8, 9.3 and 2.7–5.3 years are identified in the annual subfossil record. A comparison with the power spectra of chronologies derived from living *F. cupressoides* trees shows strong similarities with the 50,000-year-old chronology, indicating that similar growth forcing factors operated in this glacial interstadial phase as in the current interglacial conditions.

With the exception of polar and tropical ice cores and some ocean-sediment cores, palaeoclimate records with annual resolution based on studies of tree rings, coral, and varved sediments have been recovered only for the late Holocene[5]. Here we report annually resolved proxies of palaeoclimate data for southern South America for an interstadial period thought to correspond to marine oxygen isotope stage 3 (OIS 3; ref. 6). Our analysis is based on subfossil tree remnants found at Seno Reloncaví in the southern Lake District of Chile (40° 00′ to 42° 30′ S, 71° 30′ to 74° 00′ W). Here we use the term 'subfossil' to mean wood preserved since the late Pleistocene epoch that still contains carbon material. Supported by glacial geology and palynology studies, the southern Lake District represents an area where late Quaternary climate fluctuations have been best established for the entire Andes[7–10]. Although the Lake District was affected repeatedly by large ice lobes descending from the Andes at times > 14 kyr before present (BP), long-term full-glacial stratigraphic pollen records show that the forests did not completely disappear during the periods of ice advance and rapidly re-expanded afterwards[8,9]. After ice recession, evergreen forest, mainly dominated by broad-leaved and conifer elements, expanded across the Lake District with a wide ecological amplitude, from lowland floodplains to near the modern, upper tree line.

Annually resolved records in the region based on the characteristic